

# Observation of Geometric Phases in Quantum Erasers

H. Kobayashi,<sup>1</sup> S. Tamate,<sup>1</sup> T. Nakanishi,<sup>1</sup> K. Sugiyama,<sup>1</sup> and M. Kitano<sup>1</sup>

<sup>1</sup>Department of Electronic Science and Engineering, Kyoto University, Kyoto 615-8510, Japan

In this study, we report the manifestation of geometric phases in the setup for quantum erasers. Our experiment includes a double-slit interferometer with the polarization as an internal state of a photon. With regard to the visibility of the interference fringe, we can demonstrate the disappearance of fringes by which-path marking and the recovery of interference using quantum erasers, and the phase shift of the fringe due to the evolution of the polarization state is attributed to the geometric phase or the Pancharatnam phase. For a certain arrangement, the geometric phase can be very sensitive to a change in state and this is observed as a rapid displacement of the fringes.

## I. INTRODUCTION

Wave-particle duality is one of the most intriguing features of quantum mechanics. This property manifests itself prominently in the Young's double slit experiment; each quanta creates a single spot on the observation plane according to the probability amplitude, and the spots created by thousands of quanta result in a clear fringe pattern due to the superposition of wavefunctions for the two possible paths followed by the quantum particle<sup>1,2</sup>. Here, we assume that there exists a device to "mark" each particle according to the path followed by it. This operation, called as which-path marking, enables us to distinguish the two states for the path so that the superposition of the path states has been collapsed and the interference disappears.

Surprisingly, although the which-path marking destroys the interference, we can recover the interference fringe by erasing the which-path information. This idea called as the quantum eraser was first proposed by Scully and Drühl<sup>3</sup>, and it has been discussed extensively in connection with the wave-particle duality<sup>4-10</sup>.

A simple demonstration of the path marking and the quantum eraser using the internal states of a photon can be demonstrated using a double-slit interferometer as follows. A photon is marked with the right and left circular polarization states according to the paths. Because we could distinguish the path state by measuring the polarity of the circular polarization, no interference pattern is observed. However, when a linear polarizer is placed behind the double slit, the circular polarizations are projected into the same linear polarization and which-path information in the polarization state is completely erased. Therefore, the interference fringes are recovered<sup>11,12</sup>.

In addition to the recovery of interference, due to the change in the polarization states, the quantum eraser also induces an additional phase shift determined by three polarization states: two states due to the which-path marking and one due to the linear polarizer used for the quantum eraser. This phase shift is called as the Pancharatnam phase, which is proportional to the area of the spherical triangle connecting the three states on the Poincaré sphere<sup>13,14</sup>. From this geometric property, it is also called as the geometric phase<sup>15,16</sup>. It has been shown that the Pancharatnam phase can be very sensitive to a

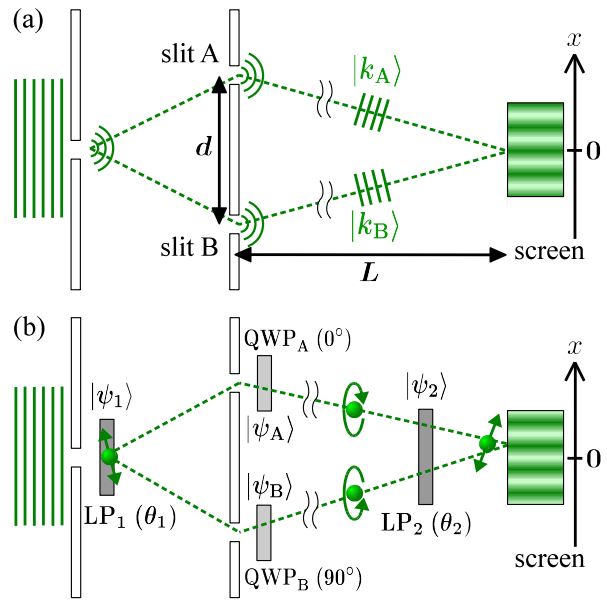


FIG. 1: (Color online). (a) A typical Young's double-slit interferometer using photons. The path states of the photon are represented as the state of the transverse wave numbers,  $|k_A\rangle$  and  $|k_B\rangle$ . (b) A double-slit interferometer with an internal state. The which-path marker comprises of the linear polarizer  $LP_1$  and the two quarter-wave plates  $QWP_A$  and  $QWP_B$ . The linear polarizer  $LP_2$  serves as the quantum eraser. The states  $|\psi_1\rangle$ ,  $|\psi_2\rangle$ ,  $|\psi_A\rangle$ , and  $|\psi_B\rangle$  are the polarization states after  $LP_1$ ,  $LP_2$ ,  $QWP_A$ , and  $QWP_B$ , respectively. The angles of the transmission axes of  $LP_1$  and  $LP_2$  are  $\theta_1$  and  $\theta_2$ , and those of the fast axes of  $QWP_A$  and  $QWP_B$  are  $0^\circ$  and  $90^\circ$ , respectively.

change in state for a certain arrangement<sup>17-21</sup>.

Recently, based on the interferometric point of view, Tamate and his co-workers revealed that the Pancharatnam phase contributes to the weak measurements<sup>22,23</sup>. In weak measurements, we can obtain unusual results that lie well outside of the range of eigenvalues of an observable. Owing to this property, the weak measurement is very useful for experimentally detecting minute effects<sup>24,25</sup>. It has been shown that the high sensitivity of the Pancharatnam phase to a change in state plays an essential role in weak measurements<sup>23</sup>.

In this study, we report the manifestation of the Pancharatnam phase in the setup for quantum erasers. The loss of interference by which-path marking can be explained by the fact that the interference pattern destroyed by the which-path marking contains two complete interference patterns that are shifted by different amounts due to the Pancharatnam phase. This is demonstrated in our experiment for a double-slit interferometer with internal states of a photon. With regard to the visibility of the interference fringe, we can confirm the disappearance of interference due to which-path marking and recovery of interference using the quantum eraser. On the other hand, we can observe the nonlinear variation of the Pancharatnam phase with regard to the phase shift of the fringe in the same setup. Although each phenomenon has already been described in previous works, in our experiment we can observe these phenomena using a single setup. It may be useful for showing a unified viewpoint of the quantum eraser and the geometric phase, and based on this viewpoint, our experiment can be interpreted as the minimal setup of weak measurement for the measured qubit (polarization states) coupled with the qubit meter (path states)<sup>26,27</sup>.

The remainder of this paper is organized as follows. In Sec. II, we introduce a theoretical model for a double-slit interferometer with the internal states and analyze the interference pattern in the process of which-path marking and the quantum eraser. Moreover, we confirm the nonlinear variation of the Pancharatnam phase in a certain arrangement. In Sec. III, we describe our experimental setup and results on the quantum eraser and the Pancharatnam phase. A summary is presented in Sec. IV.

## II. THEORETICAL ANALYSIS OF DOUBLE-SLIT INTERFEROMETERS WITH INTERNAL STATES

An interferometer with internal states can be analyzed as a quantum system composed of the path state and the internal state. In this section, we theoretically analyze the interference patterns in our double-slit experiment with regard to both the intensity and the phase.

### A. Which-path marking

Because of the large distance between the double slit and the screen, the state of the photon through slits A and B can be assumed to be an eigenstate of the transverse wave numbers on the screen,  $|k_A\rangle$  and  $|k_B\rangle$ , respectively, as shown in Fig. 1(a). These states satisfy the normalization condition  $\langle k|k' \rangle = \delta(k - k')$ , where  $\delta(\cdot)$  shows the Dirac delta function. In our setup, a photon is marked with the polarization states  $|\psi_A\rangle$  and  $|\psi_B\rangle$  according to the paths using the quarter-wave plates QWP<sub>A</sub> and QWP<sub>B</sub> (see Fig. 1(b)). Assuming that the photon has a 50:50 chance of passing through each slit,

the total state vector for the composite system can be represented as the following superposition:

$$|\Psi_m\rangle = |\psi_A\rangle|k_A\rangle + |\psi_B\rangle|k_B\rangle. \quad (1)$$

Here, the path states and two polarization states are correlated or *entangled*. We introduce the operator  $\hat{P}_x \equiv \hat{I} \otimes |x\rangle\langle x|$ , which projects the path state into the position state  $|x\rangle$  on the screen. With the position representation of the wave-number eigenfunction,  $\langle x|k\rangle = e^{ikx}/\sqrt{2\pi}$ , the probability distribution  $P_m(x)$  is given by

$$P_m(x) = \langle \Psi_m | \hat{P}_x | \Psi_m \rangle \propto 1 + V_m \cos(kx - \delta_m), \quad (2)$$

where  $k \equiv k_B - k_A$  and

$$V_m = |\langle \psi_B | \psi_A \rangle|, \quad (3)$$

$$\delta_m = \arg \langle \psi_B | \psi_A \rangle. \quad (4)$$

For the double-slit apparatus,  $k$  is calculated as  $k = 2\pi d/\lambda L$ , where  $\lambda$  is the wavelength of light;  $d$ , the distance between two slits; and  $L$ , the distance between the double slit and the screen. The coefficient of the interference term,  $V_m$ , can be experimentally obtained from the fringe pattern as the visibility

$$V_m = \frac{P_{\max} - P_{\min}}{P_{\max} + P_{\min}}, \quad (5)$$

where  $P_{\max}$  and  $P_{\min}$  are the maximum and minimum values of  $P_m(x)$ , respectively.

The degradation of visibility is related to the efficacy of which-path marking, which depends on the inner product  $\langle \psi_A | \psi_B \rangle$ . The lesser the value of  $|\langle \psi_A | \psi_B \rangle|$ , the lesser is the visibility. In particular, when  $\langle \psi_A | \psi_B \rangle = 0$ , two states are perfectly distinguishable and the path followed by the photon is discriminated unambiguously. Then, the interference is completely eliminated.

### B. Quantum eraser

Now, we erase the which-path information by the projection of polarization using the linear polarizer LP<sub>2</sub> that projects the polarization state into  $|\psi_2\rangle$  (see Fig. 1(b)). The state vector for the composite system after LP<sub>2</sub> is calculated as follows:

$$|\Psi_f\rangle = |\psi_2\rangle\langle\psi_2|\Psi_m\rangle = |\psi_2\rangle\left(c_A|k_A\rangle + c_B|k_B\rangle\right), \quad (6)$$

where  $c_A = \langle\psi_2|\psi_A\rangle$  and  $c_B = \langle\psi_2|\psi_B\rangle$ . The probability distribution  $P_f(x)$  is given by

$$P_f(x) = \langle \Psi_f | \hat{P}_x | \Psi_f \rangle \propto 1 + V_f \cos(kx - \delta_f), \quad (7)$$

where the visibility  $V_f$  and the phase shift  $\delta_f$  are given as

$$V_f = \frac{2|c_A| \cdot |c_B|}{|c_A|^2 + |c_B|^2}, \quad (8)$$

$$\delta_f = \arg \langle \psi_B | \psi_2 \rangle \langle \psi_2 | \psi_A \rangle. \quad (9)$$

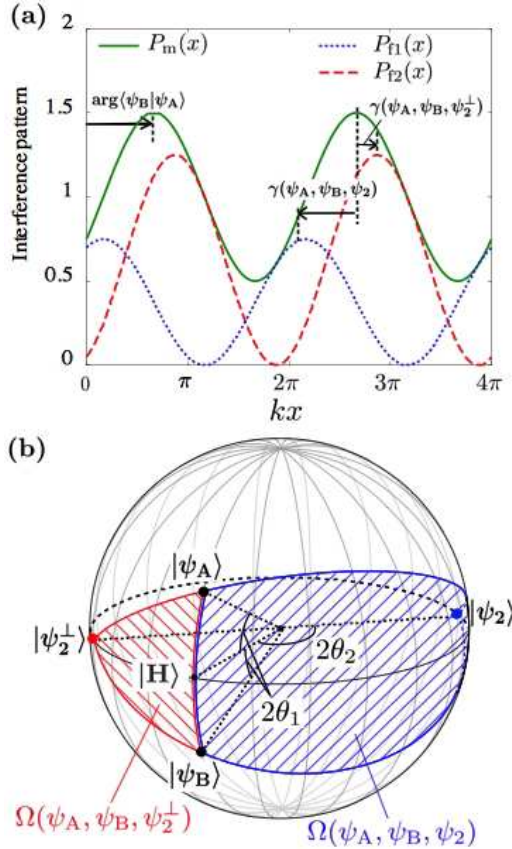


FIG. 2: (Color online). Separation of the partial interference pattern. (a) The partial interference pattern can be separated into two fringes with 100% visibility shifted by  $\gamma(\psi_A, \psi_B, \psi_2)$  and  $\gamma(\psi_A, \psi_B, \psi_2^\perp)$ . (b) The shifts are related to the solid angles of the spherical triangles on the Poincaré sphere as  $\gamma(\psi_1, \psi_2, \psi_3) = -\frac{1}{2}\Omega(\psi_1, \psi_2, \psi_3)$ .

Equation (8) shows that even when  $|\psi_A\rangle$  is orthogonal to  $|\psi_B\rangle$ , the visibility is recovered completely provided that  $|c_A| = |c_B|$ . In this case, the states of the which-path marker,  $|\psi_A\rangle$  and  $|\psi_B\rangle$ , are projected into the same polarization state  $|\psi_2\rangle$  with the same probability, and it cannot be determined whether the photon came from slit A or B. This implies that LP<sub>2</sub> completely erases the which-path information, and the interference is recovered.

### C. Quantum eraser and Pancharatnam phase

As shown in the previous section, the which-path marker can destroy the interference pattern effectively. However, using the quantum eraser, the interference can be restored completely. This implies that the complete interference pattern is buried under the destroyed interference pattern. In this section, we will show that the interference pattern destroyed by the which-path marking contains two complete interference patterns that are shifted by different amounts according to the projection

of the polarization state. These phase shifts can be interpreted geometrically using the Poincaré sphere, as shown below.

Equation (2) can be separated into two terms using the projected state  $|\psi_2\rangle$  that satisfies  $|\langle\psi_2|\psi_A\rangle| = |\langle\psi_2|\psi_B\rangle|$  and its orthogonal state  $|\psi_2^\perp\rangle$  as follows:

$$P_m(x) = \langle\Psi|[(|\psi_2\rangle\langle\psi_2| + |\psi_2^\perp\rangle\langle\psi_2^\perp|) \otimes |x\rangle\langle x|]|\Psi\rangle \propto |c_A|^2 P_{f1}(x) + (1 - |c_A|^2) P_{f2}(x), \quad (10)$$

with

$$P_{f1}(x) \equiv 1 + \cos[kx - \delta_m - \gamma(\psi_A, \psi_B, \psi_2)], \quad (11)$$

$$P_{f2}(x) \equiv 1 + \cos[kx - \delta_m - \gamma(\psi_A, \psi_B, \psi_2^\perp)], \quad (12)$$

where the additional phase shift  $\gamma$  is defined as

$$\gamma(\psi_1, \psi_2, \psi_3) \equiv \arg\langle\psi_1|\psi_2\rangle\langle\psi_2|\psi_3\rangle\langle\psi_3|\psi_1\rangle. \quad (13)$$

Due to the difference in the phase shifts,  $\gamma(\psi_A, \psi_B, \psi_2) - \gamma(\psi_A, \psi_B, \psi_2^\perp)$ , even though both fringes  $P_{f1}(x)$  and  $P_{f2}(x)$  have 100% visibility, the sum of these patterns has reduced visibility [see Fig. 2(a)].

The right-hand side of Eq. (13) is gauge-invariant, i.e., independent of the choice of the phase factor of each state, because the bra and ket vectors for each state appear in a pair. This phase shift  $\gamma$  is identified with the Pancharatnam phase<sup>13</sup>. It can be shown that the Pancharatnam phase is proportional to the solid angle  $\Omega(\psi_1, \psi_2, \psi_3)$  of the spherical triangle connecting the states  $|\psi_1\rangle$ ,  $|\psi_2\rangle$ , and  $|\psi_3\rangle$  with geodesic arcs on the Poincaré sphere<sup>13,14</sup>, i.e.,

$$\gamma(\psi_1, \psi_2, \psi_3) = -\frac{1}{2}\Omega(\psi_1, \psi_2, \psi_3). \quad (14)$$

Therefore, each phase shift of two fringes,  $\gamma(\psi_A, \psi_B, \psi_2)$  and  $\gamma(\psi_A, \psi_B, \psi_2^\perp)$ , can be represented geometrically on the Poincaré sphere. When the two marker states  $|\psi_A\rangle$  and  $|\psi_B\rangle$  are located along a meridian symmetric with respect to the equator, the projected states  $|\psi_2\rangle$  and  $|\psi_2^\perp\rangle$  should be on the equator in order to satisfy the condition  $|\langle\psi_2|\psi_A\rangle| = |\langle\psi_2|\psi_B\rangle|$ , as shown in Fig. 2(b).

In particular, if  $|\psi_A\rangle$  is perpendicular to  $|\psi_B\rangle$ , that is, a 100%-effective which-path marker is prepared, the four states  $|\psi_A\rangle$ ,  $|\psi_B\rangle$ ,  $|\psi_2\rangle$ , and  $|\psi_2^\perp\rangle$  lie on the same great circle. Then, the following equation is satisfied:

$$\gamma(\psi_A, \psi_B, \psi_2) - \gamma(\psi_A, \psi_B, \psi_2^\perp) = \pi, \quad |c_A|^2 = \frac{1}{2}. \quad (15)$$

The total pattern is composed of two fringes having the same intensity but opposite phases, and the interference is completely washed out. A general case of partial erasure is shown in Fig. 2.

### D. Nonlinear variation of Pancharatnam phase

From Eq. (14), we can calculate the Pancharatnam phase in our experiments. We modify the standard

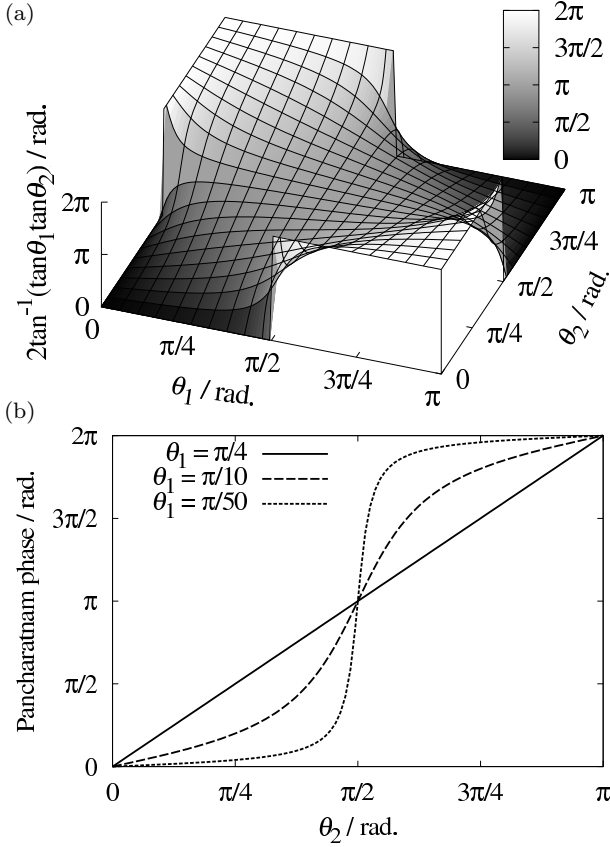


FIG. 3: Variation of the Pancharatnam phase (a) with respect to  $\theta_1$  and  $\theta_2$ , and (b) with respect to  $\theta_2$  for different  $\theta_1$ .

double-slit interferometer to include two linear polarizers and two quarter-wave plates, as shown in Fig. 1(b).

First, we prepare the initial polarization state  $|\psi_1\rangle$  using the linear polarizer LP<sub>1</sub> :

$$|\psi_1\rangle = \cos \theta_1 |H\rangle + \sin \theta_1 |V\rangle, \quad (16)$$

where  $\theta_1$  is the angle between the horizontal line and the transmission axis of LP<sub>1</sub>;  $|H\rangle$ , the horizontal polarization state; and  $|V\rangle$ , the vertical polarization state. In our setup, the fast axes of two quarter-wave plates, QWP<sub>A</sub> and QWP<sub>B</sub>, are aligned to form angles of 0° and 90°, respectively, from the horizontal line. Thus, they induce phase shifts of  $\pm\pi/2$  between the horizontal and the vertical components:

$$|\psi_A\rangle = \cos \theta_1 |H\rangle + i \sin \theta_1 |V\rangle, \quad (17)$$

$$|\psi_B\rangle = i \cos \theta_1 |H\rangle + \sin \theta_1 |V\rangle. \quad (18)$$

Here, the pair of quarter-wave plates serves as the which-path marker in Eq. (1). The final state of the polarization is expressed as  $|\psi_2\rangle$ :

$$|\psi_2\rangle = \cos \theta_2 |H\rangle + \sin \theta_2 |V\rangle, \quad (19)$$

where  $\theta_2$  is the angle between the horizontal line and the transmission axis of LP<sub>2</sub>.

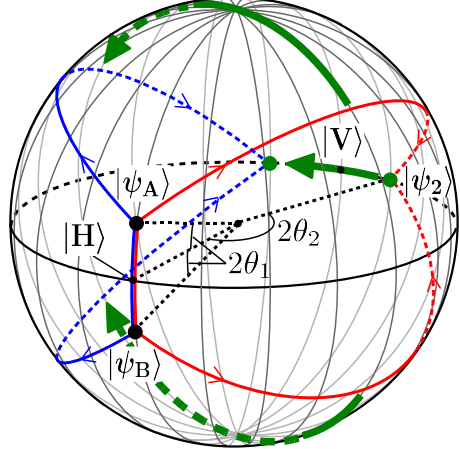


FIG. 4: (Color online). Geometrical interpretation of the non-linear variation of the Pancharatnam phase around  $(\theta_1, \theta_2) = (0, \pi/2)$ . If  $|\psi_A\rangle$  and  $|\psi_B\rangle$  are close to each other on the Poincaré sphere, the area of the spherical triangle blows up very rapidly with the movement of  $|\psi_2\rangle$  around  $\theta_2 = \pi/2$ .

From Eqs. (17), (18), and (19), we can obtain the Pancharatnam phase as

$$\gamma(\psi_A, \psi_B, \psi_2) = \begin{cases} 2 \tan^{-1}(\tan \theta_1 \tan \theta_2) & (\cos 2\theta_1 \geq 0), \\ 2 \tan^{-1}(\tan \theta_1 \tan \theta_2) + \pi & (\cos 2\theta_1 < 0). \end{cases} \quad (20)$$

Figure 3(a) shows the variation of the first term of Eq. (20) with respect to  $\theta_1$  and  $\theta_2$ . It is noteworthy that this variation exhibits strong nonlinearity around  $(\theta_1, \theta_2) = (0, \pi/2)$ ,  $(\pi/2, 0)$ ,  $(\pi/2, \pi)$ , and  $(\pi, \pi/2)$ . In Fig. 3(b), the variation of the Pancharatnam phase with  $\theta_2$  is plotted for different values of  $\theta_1$ . The figure shows that the smaller the value of  $\theta_1$ , the faster is the change in the Pancharatnam phase with respect to  $\theta_2$  near  $\theta_2 = \pi/2$ . We can observe this nonlinear variation as a rapid displacement of the fringes when we change  $\theta_2$  by rotating LP<sub>2</sub>.

The nonlinear variation of the Pancharatnam phase can be explained by the spherical geometry on the Poincaré sphere, as shown in Fig. 4. In our experiment,  $|\psi_A\rangle$  and  $|\psi_B\rangle$ , given by Eqs. (17) and (18), respectively, can be depicted at a latitude of  $\pm\theta_1$  on the prime meridian, and the final state  $|\psi_2\rangle$ , given by Eq. (19), can be depicted on the equator at a longitude of  $2\theta_2$ . We assume that  $|\psi_A\rangle$  and  $|\psi_B\rangle$  are located near  $|H\rangle$ , that is,  $0 < \theta_1 \ll \pi/4$  is satisfied, and  $|\psi_2\rangle$  moves on the equator from  $|H\rangle$ . When the distance between  $|\psi_2\rangle$  and  $|V\rangle$  is greater than  $2\theta_1$ , the area of the spherical triangle spanned by  $|\psi_A\rangle$ ,  $|\psi_B\rangle$ , and  $|\psi_2\rangle$  remains small. However, when  $|\psi_2\rangle$  approaches  $|V\rangle$  and the distance between them becomes lesser than  $2\theta_1$ , the area of the spherical triangle increases very rapidly, and after traversing  $|V\rangle$ , the triangle covers most of the Poincaré sphere. This is

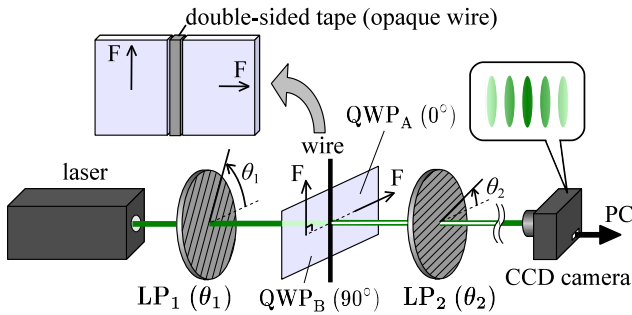


FIG. 5: (Color online). Experimental setup for double-slit quantum eraser. Light passing through the right and left of the wire interferes. Each path is marked by two film-type quarter-wave plates,  $QWP_A$  and  $QWP_B$ , whose fast axes  $F$  make angles of  $0^\circ$  and  $90^\circ$ , respectively. The interference fringe is captured using a CCD camera.

the geometrical reasoning why the Pancharatnam phase changes rapidly in certain conditions.

### III. EXPERIMENTS

The experimental setup is shown in Fig. 5. The light source is a 532-nm green laser with a 3-mm beam diameter (model DPGL-2200, SUWTECH). A thin opaque wire crossing the beam works as the double slit; the light passing through the right- and left-hand sides of the wire interferes due to diffraction. We attached two film-type quarter-wave plates having the orthogonal fast axes,  $0^\circ$  and  $90^\circ$ , with a thin piece of double-sided adhesive tape that works as a wire. A double slit having a similar design has been introduced by Hilmer and Kwiat<sup>12</sup>.

Two film-type linear polarizers,  $LP_1$  and  $LP_2$ , are attached to the rotatable mounts with graduated scales for adjusting the angles  $\theta_1$  and  $\theta_2$ . At a distance of approximately 1 m from the double slit, the recombined beam is captured using a charge-coupled device (CCD) camera (model LBP-2-USB, Newport) connected to a personal computer (PC). The CCD camera has a resolution of  $640 \times 480$  pixels, each having a size of  $9 \mu\text{m} \times 8 \mu\text{m}$ , and it is equipped with a gain controller.

#### A. Experimental results of quantum erasers

First, by setting  $\theta_1 = \pi/4$  and removing the linear polarizer  $LP_2$ , the initial state of polarization  $|D\rangle$  is evolved into two orthogonal states through the quarter-wave plates, right circular polarization, and left circular polarization according to the paths. Because we can determine which slit the photon has passed through by measuring the polarity of the circular polarization of the photon, no interference pattern is obtained. (This is mathematically confirmed from Eq. (3), which vanishes

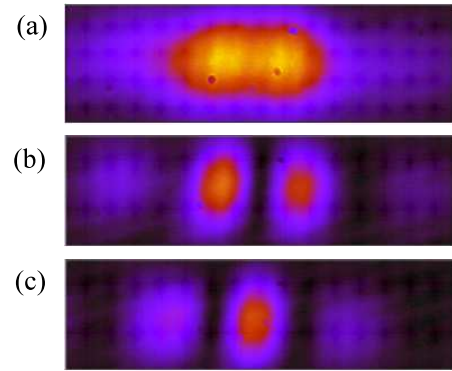


FIG. 6: (Color online). Interference patterns captured using a CCD camera. (a) By setting  $\theta_1 = \pi/4$  and removing  $LP_2$ , a typical diffraction pattern is observed. (b) By setting  $\theta_1 = \pi/4$  and  $\theta_2 = 0$ , the fringe pattern reappears. (c) By setting  $\theta_1 = \pi/4$  and  $\theta_2 = \pi/2$ , the fringe pattern is out of phase with the case of  $\theta_2 = 0$ .

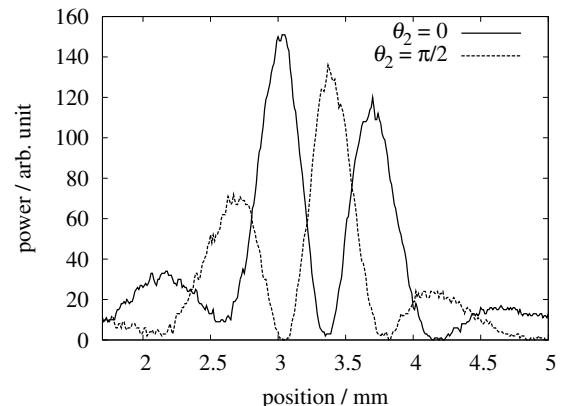


FIG. 7: Recovered interference fringes for the quantum eraser with  $\theta_2 = 0$  and  $\theta_2 = \pi/2$

when  $|\psi_A\rangle$  is orthogonal to  $|\psi_B\rangle$ .) We observed a typical diffraction pattern that only has broad peaks, as shown in Fig. 6(a).

By inserting  $LP_2$ , the right and left circular polarizations are projected into the same linear polarization with the same probability, and therefore, the polarization provides no which-path information. As a result, the interference fringe reappears. (Mathematically, this corresponds to the fact that Eq. (8) becomes unity when  $|c_A| = |c_B|$ .) Figure 6(b) shows the recovered interference fringe for  $\theta_2 = 0$ . Similarly, for  $\theta_2 = \pi/2$ , we can obtain the corresponding interference fringe, as shown in Fig. 6(c), which is out of phase with that observed for  $\theta_2 = 0$  (see Fig. 7). This phase difference is attributed to the Pancharatnam phase. The sum of these interference patterns reproduces the broad peak pattern, as shown in Fig. 6(a), that is obtained in the absence of  $LP_2$ . Therefore, the quantum eraser actually filters out one of these

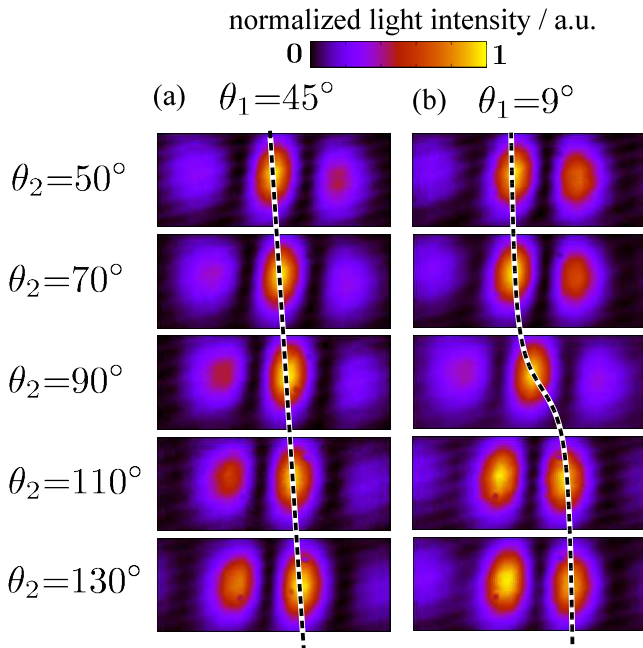


FIG. 8: (Color online). The shift of fringes induced by the Pancharatnam phase with respect to  $\theta_2$  (a) when  $\theta_1 = 45^\circ$  and (b) when  $\theta_1 = 9^\circ$ . The light intensity of each frame is normalized individually. When  $\theta_1 = 9^\circ$ , the fringe exhibits a rapid displacement around  $\theta_2 = 90^\circ$ .

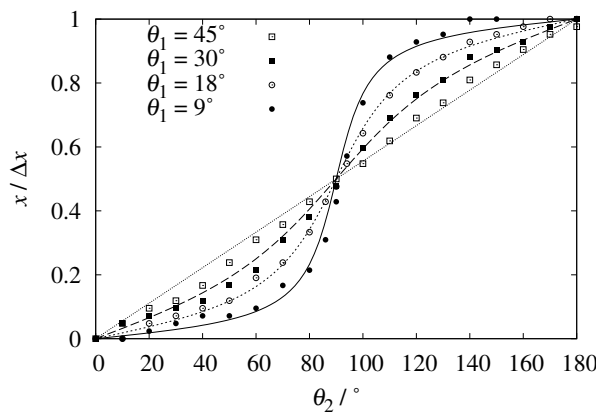


FIG. 9: Experimental results of Pancharatnam phase with respect to  $\theta_2$  for different  $\theta_1$ . The vertical axis shows the displacement of the fringe normalized by the spatial period of the fringe.

fringes and perfectly recovers the visibility.

### B. Observation of Pancharatnam phase and its nonlinearity

In order to observe the variation of the Pancharatnam phase with respect to  $\theta_1$  and  $\theta_2$ , we measured the dis-

placement of the fringes. Figure 8 shows the fringe shift with respect to  $\theta_2$  for fixed  $\theta_1$ . The light intensity of each fringe in Fig. 8 is normalized individually. When  $\theta_1 = 45^\circ$ , the fringe moves linearly with respect to the change in  $\theta_2$ , as shown in Fig. 8(a). However, setting  $\theta_1 = 9^\circ$ , the fringe exhibits a quick displacement around  $\theta_2 = 90^\circ$ , as shown in Fig. 8(b).

Figure 9 shows the variation of the Pancharatnam phase with respect to  $\theta_2$  for  $\theta_1 = 45^\circ$ ,  $30^\circ$ ,  $18^\circ$ , and  $9^\circ$ . The points in Fig. 9 indicate the experimental results and the solid lines indicate the theoretical lines calculated using Eq. (20). The vertical axis is the displacement of the fringe  $x$  normalized by the spatial period of the fringe  $\Delta x$ . The origin of the vertical axis is determined by the position of the fringes when  $\theta_2 = 0^\circ$ . All the experimental results agree well with the theoretical ones. The gradient of the variation of the shift around  $\theta_2 = 90^\circ$  increases as  $\theta_1$  is decreased. This implies that the variation of the shift becomes more sensitive to the variation of the last polarization state.

### IV. SUMMARY

We have shown that the Pancharatnam phase manifests in the setup for quantum erasers. In our experiment, we have introduced a double-slit interferometer with internal states of a photon and demonstrated which-path marking, quantum erasers, and the variation of the geometric phases. The visibility of the interference fringe is related to the which-path marking and the quantum eraser, and the phase shift of the interference shows the manifestation of the Pancharatnam phase. Moreover, we have demonstrated that the Pancharatnam phase could become sensitive to a change in the polarization state. This fact can be utilized for high-precision measurement of the polarization.

Even though our experiment is performed with classical light, it serves the purpose of showing the quantum-mechanical meaning of which-path marking, quantum erasers, and geometric phases since photons are noninteracting Bose particles and our tests can be straightforwardly extended to experiments with single photons<sup>28</sup>.

### Acknowledgments

We gratefully thank Youhei Hosoe for assisting us in our experiments. We thank Yosuke Nakata and Rikizo Ikuta for providing useful comments and suggestions. This research is supported by the global COE program “Photonics and Electronics Science and Engineering” at Kyoto University.

---

<sup>1</sup> S. Parker: Am. J. Phys. **40** (1972) 1003.

<sup>2</sup> W. Rueckner and P. Titcomb: Am. J. Phys. **64** (1996) 184.

<sup>3</sup> M. O. Scully and K. Drühl: Phys. Rev. A **25** (1982) 2208.

<sup>4</sup> S. M. Tan and D. F. Walls: Phys. Rev. A **47** (1993) 4663.

<sup>5</sup> T. J. Herzog, P. G. Kwiat, H. Weinfurter, and A. Zeilinger: Phys. Rev. Lett. **75** (1995) 3034.

<sup>6</sup> B. G. Englert: Phys. Rev. Lett. **77** (1996) 2154.

<sup>7</sup> A. Luis and L. L. Sánchez-Soto: Phys. Rev. Lett. **81** (1998) 4031.

<sup>8</sup> G. Björk and A. Karlsson: Phys. Rev. A **58** (1998) 3477.

<sup>9</sup> P. D. D. Schwindt, P. G. Kwiat, and B. G. Englert: Phys. Rev. A **60** (1999) 4285.

<sup>10</sup> S. P. Walborn, M. O. T. Cunha, S. Pádua, and C. H. Monken: Phys. Rev. A **65** (2002) 033818.

<sup>11</sup> S. P. Walborn, M. O. T. Cunha, S. Pádua, and C. H. Monken: Am. Sci. **91** (2003) 336.

<sup>12</sup> R. Hillmer and P. Kwiat: Sci. Am. **296** (2007) 72.

<sup>13</sup> S. Pancharatnam: Proc. Ind. Acad. Sci. A **44** (1956) 247.

<sup>14</sup> P. K. Aravind: Opt. Commun. **94** (1992) 191.

<sup>15</sup> M. V. Berry: Proc. R. Soc. London A **392** (1984) 45.

<sup>16</sup> M. V. Berry: J. Mod. Opt. **34** (1987) 1401.

<sup>17</sup> H. Schmitzer, S. Klein, and W. Dultz: Phys. Rev. Lett. **71** (1993) 1530.

<sup>18</sup> S. P. Tewari, V. S. Ashoka, and M. S. Ramana: Opt. Commun. **120** (1995) 235.

<sup>19</sup> R. Bhandari: Phys. Rep. **281** (1997) 1.

<sup>20</sup> B. Hils, W. Dultz, and W. Martienssen: Phys. Rev. E **60** (1999) 2322.

<sup>21</sup> Q. Li, L. Gong, Y. Gao, and Y. Chen: Opt. Commun. **169** (1999) 17.

<sup>22</sup> Y. Aharonov, D. Z. Albert, and L. Vaidman: Phys. Rev. Lett. **60** (1988) 1351.

<sup>23</sup> S. Tamate, H. Kobayashi, T. Nakanishi, K. Sugiyama, and M. Kitano: New J. Phys. **11** (2009) 093025.

<sup>24</sup> O. Hosten and P. Kwiat: Science **319** (2008) 787.

<sup>25</sup> P. B. Dixon, D. J. Starling, A. N. Jordan, and J. C. Howell: Phys. Rev. Lett. **102** (2009) 173601.

<sup>26</sup> T. A. Brun, L. Diósi, and W. T. Strunz: Phys. Rev. A **77** (2008) 032101.

<sup>27</sup> S. Wu and K. Mølmer: Phys. Lett. A **374** (2009) 34.

<sup>28</sup> R. Y. Chiao and Y.-S. Wu: Phys. Rev. Lett. **57** (1986) 933.